Electronic Supplementary Material (ESI) for Journal of Materials Chemistry B.

Supporting Information

Interactions of Nitroxide Radicals with Dendrimer-entrapped Au_8-clusters: A Fluorescent Nanosensor for Intracellular Imaging of Ascorbic Acid

Ching-Ping Liu, Te-Haw Wu, Chia-Yeh Liu, and Shu-Yi Lin*

Institute of Biomedical Engineering and Nanomedicine, National Health Research Institutes, 35 Keyan Road, Zhunan 350, Taiwan

The detailed calculation of V (the static quenching constant) and K_{SV} (equal to K_D, the dynamic quenching constant) in the modified Stern-Volmer eqn (1):

As shown in Fig. 1b, it is apparent that the ratio of F_0/F gives an upward curving plot. By treating the data according to the modified Stern-Volmer eqn. (1), plotting $F_0/\text{Fexp}(V[Q])$ vs. [Q] for varying V until a linear plot is obtained and then giving a V of 18 M^{-1} (equal to 0.018 mM^{-1}). After that, the linear plot of $F_0/\text{Fexp}(0.018[Q])$ against [Q] represents correction for static quenching of the steady-state fluorescence (red dots in Fig. 1b) and its slope was observed, giving a K_{SV} (=K_D) of 23 M^{-1} (equal to 0.023 mM^{-1}).

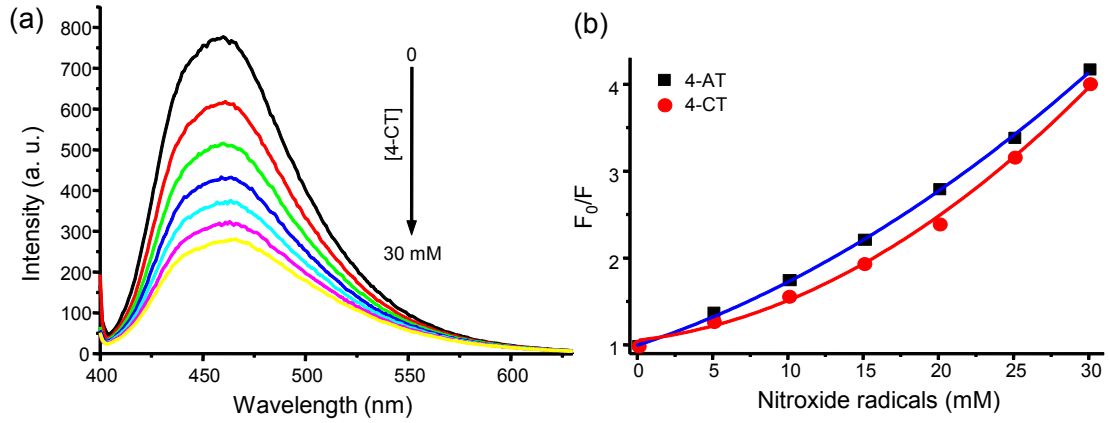

Fig. S1 (a) Changes in the fluorescence spectra of the Au_8-cluster solution (0.25 mM) resulting from the addition of various concentrations of 4-CT (0-30 mM) were measured at an excitation wavelength of 390 nm. (b) Fluorescence quenching curves of the Au_8-cluster yielded by the addition of various concentrations of 4-AT (blue line) and 4-CT (red line), respectively.

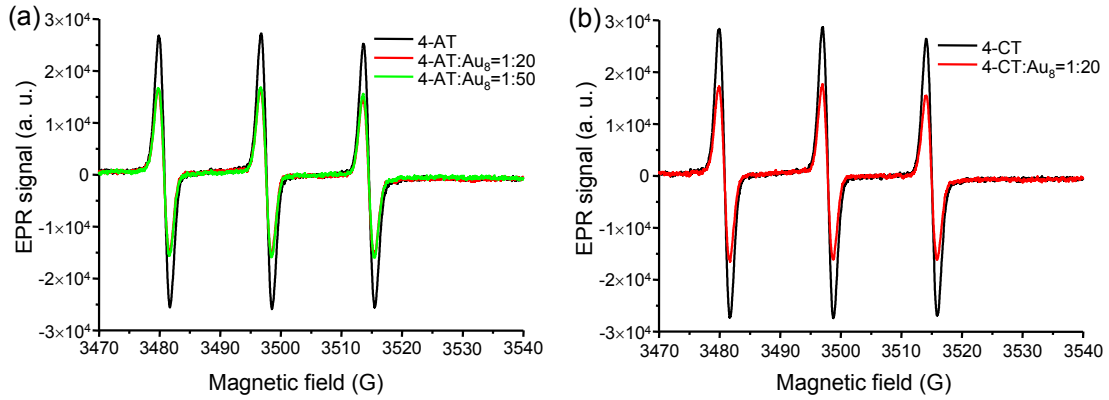

Fig. S2 EPR spectra of aqueous solutions prepared with (a) 4-AT and two molar ratios of 4-AT/Au_8-clusters (fixed [4-AT]=1.0 μM); (b) 4-CT and the molar ratio of 4-CT/the Au_8-cluster as 1:20, respectively.

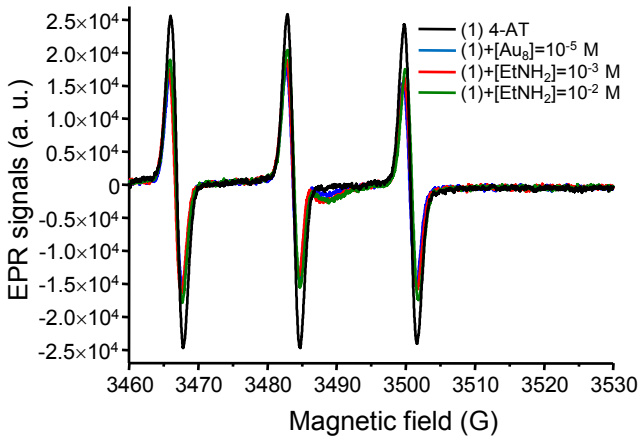

Fig. S3 EPR spectra of aqueous solutions prepared with 4-AT of 1.0 μM as solution (1), solution (1) + $[Au_8]=10^{-5}$ M, solution (1) + $[EtNH_2]=10^{-3}$ M, and solution (1) + $[EtNH_2]=10^{-2}$ M, respectively.

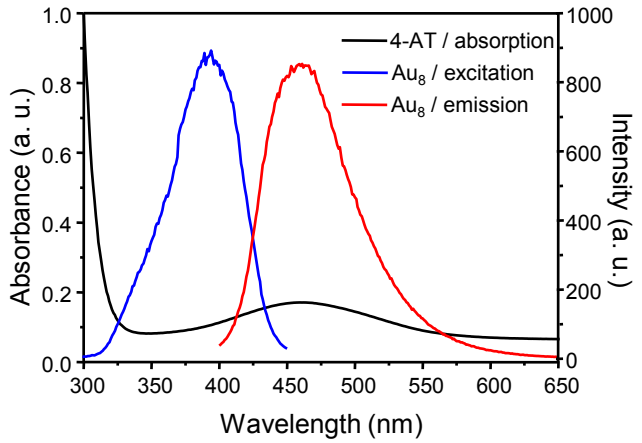

Fig. S4 Comparison of the absorption spectrum for 4-AT and the excitation and emission spectra of the Au_8-cluster in aqueous solutions.

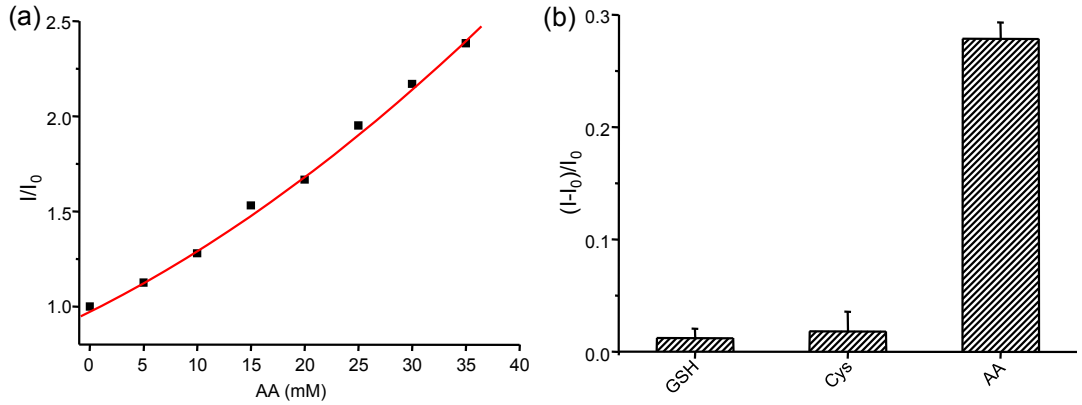

Fig. S5 The fluorescence restoration curve of the mixture (Au_8-clusters + 4-AT) yielded by the addition of various concentrations of AA (0-35 mM). (b) Relative fluorescence intensities $(I-I_0)/I_0$ at emission of 460 nm from the mixture of Au_8-clusters and 4-AT after the addition of GSH, Cys, and AA, respectively.

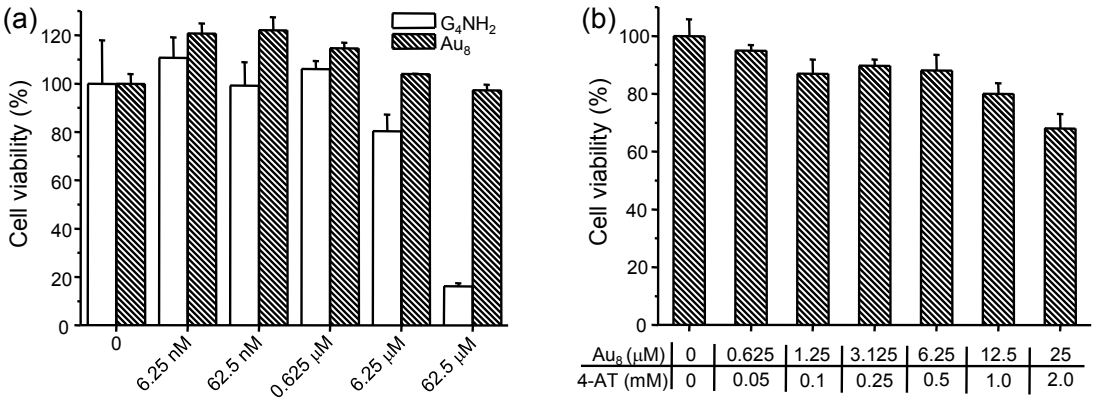

Fig. S6 Cell viability of (a) A549 cells incubated with dendrimers (G_4NH_2) and Au_8-clusters, respectively (referred to our previous work in ref. 14), and (b) MDA-MB-231 cells incubated with the mixture of Au_8-clusters and 4-AT (molar ratio 1:80) at different concentrations for 24 h.

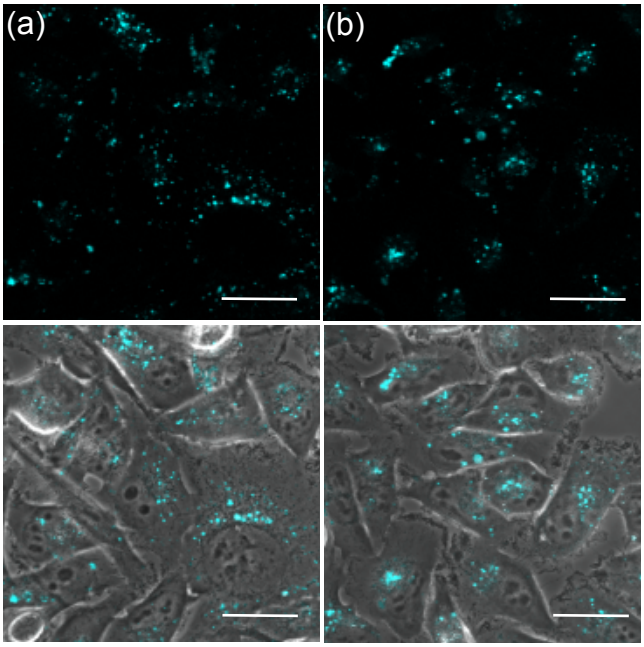

Fig. S7 The confocal fluorescence images (upper panels) and their merged transmission images (lower panels) of MDA-MB-231 breast cancer cells treated with (a) Au_8-clusters (0.5 μM) and (b) Au_8-clusters (0.5 μM) mixing with AA (5.0 mM) for 16 h, respectively. The scale bars are 30 μm.

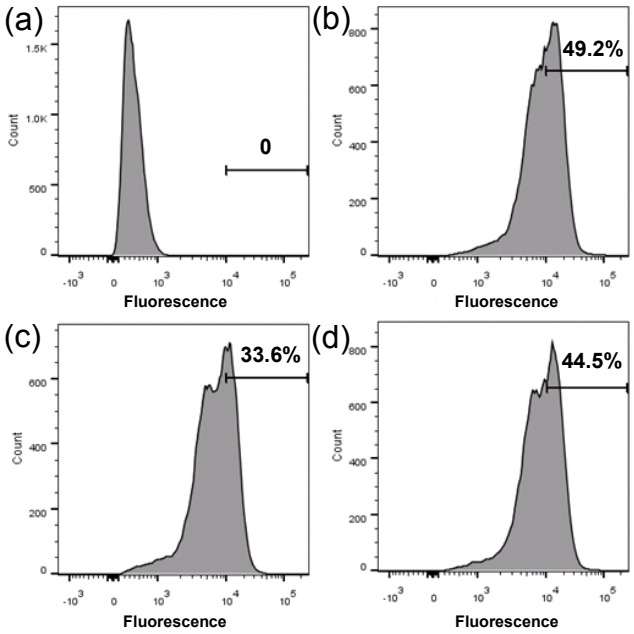

Fig. S8 Flow cytometric analysis was used to calculate the percent of gated cells for (a) cells without treatment as control and (b) cells treated with Au_8-clusters, (c) Au_8+4-AT and (d) Au_8+4-AT+AA, respectively.

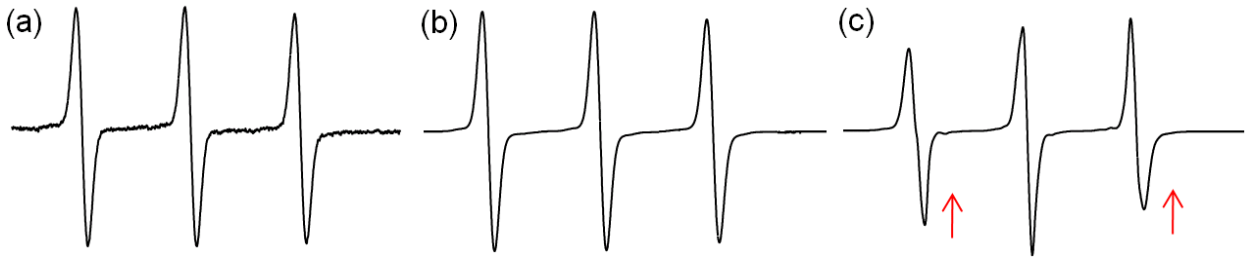

Fig. S9 Comparison of EPR spectra for samples containing the following: (a) the aqueous solution of 4-AT, (b) the solution of 4-AT and Au_8-clusters with O_2 purge for 10 min and the reaction then maintained for one week, and (c) the mixture of 4-AT and 4-OT (with a molar ratio of 1:0.2). Note that asymmetry is appeared, indicative of a mixture of nitroxide radicals including 4-AT and 4-OT.